The Journal of Chemical Physics ARTICLE scitation.org/journal/jcp

Electronic spectroscopy of carbon chains (C_{2n+1}, n = 7–10) of astrophysical importance. I. Quantum chemistry

Cite as: J. Chem. Phys. 151, 054303 (2019); doi: 10.1063/1.5108725
Submitted: 1 May 2019 • Accepted: 26 June 2019 •
Published Online: 2 August 2019

S. Rajagopala Reddy,[a] Arpita Ghosh, and S. Mahapatra[b]

AFFILIATIONS

School of Chemistry, University of Hyderabad, Hyderabad 500 046, India

[a]**Present address:** Department of Computational Sciences, Central University of Punjab, Bathinda 151001, India.
[b]**Author to whom correspondence should be addressed:** susanta.mahapatra@uohyd.ac.in

ABSTRACT

Carbon chains have been predicted to be potential carriers of diffuse interstellar band features in astrophysical observations. Motivated by numerous predictions, we set out to carry out extensive *ab initio* quantum chemistry calculations to establish the ground and excited electronic potential energy surfaces and their coupling surfaces for carbon chains containing an odd number of carbon atoms (C_{2n+1}, n = 7–10). Vibronic coupling models are established with the aid of the calculated electronic energies to investigate nuclear dynamics from first principles. The latter are reported in Ghosh *et al.* [J. Chem. Phys. **151**, 054304 (2019)]. The mentioned carbon chains possess a linear cumulenic structure at the equilibrium minimum of their electronic ground state, and an electronic excited state of the $^1\Sigma_u^+$ term appears to be extremely bright optically and absorbs in the visible region of the electromagnetic spectrum. Vertical excitation energy of this state decreases and transition dipole moment increases, and as a result, the oscillator strength of this state linearly increases with an increase of the chain length. There are states belonging to $^1\Pi_g$, $^1\Pi_u$, $^1\Sigma_g^+$, $^1\Delta_g$, and $^1\Delta_u$ terms, in the immediate vicinity of the $^1\Sigma_u^+$ state, which are optically dark but can gain intensity through vibronic coupling with the optically bright $^1\Sigma_u^+$ state. Construction of a coupling scheme considering the Renner-Teller coupling within the degenerate Π states and pseudo-Renner-Teller coupling between the Renner-Teller split component states as well as with the nondegenerate Σ states is another motivation of this work. The coupled-state Hamiltonian is constructed in a diabatic electronic basis in terms of the dimensionless normal coordinates of the vibrational modes of the carbon chains. Both Renner-Teller and pseudo-Renner-Teller types of couplings are included in the Hamiltonian. The theoretical results are discussed in relation to the experimental findings.

I. INTRODUCTION

The electronic structure and absorption spectroscopy of neutral carbon clusters received renewed attention in the literature because of their apparent importance in the spectroscopy of interstellar space.[1,2] The first spectroscopic detection of C_3 in comets in 1881 triggered curiosity among the stellar as well as laboratory spectroscopists to identify neutral carbon clusters as carriers of diffuse interstellar bands (DIBs).[3,4] Douglas in a seminal paper suggested that the carbon chains, C_n, where n may lie in the range of 5–15, may show spectroscopic features consistent with DIBs.[5] The diffuse structure of these bands was attributed to a short lifetime of excited electronic states of the carrier molecules.[6]

Following the above development, many experimental and computational studies were carried out on anionic, neutral, and cationic carbon clusters.[7–12] In this context, two reviews, covering the rich history of carbon clusters, by Weltner[13] and Van Orden[14] are noteworthy. Smaller carbon clusters were predicted to have linear equilibrium geometry with a cumulenic (:C=C=C=C:) type of bonding with nearly equal C—C bond lengths. Linear chains with an odd number of carbon atoms were predicted to have a $^1\Sigma_g^+$ electronic ground term in contrast to a $^3\Sigma_g^-$ electronic ground term for the cluster chains with an even number of carbon atoms.[13,14] Cluster chains longer than C_{10} were proposed to have ring structures as well, because of the reduction of ring strain and added stability due to the

formation of an extra C—C bond.[13,14] However, the cyclic clusters are reported to be difficult to detect and characterize spectroscopically.[13,14] Therefore, the linear cluster chains are discussed in the majority of the experiments.[15,16] The clusters, C_{2n+1} (n = 7–10), seem to have a linear cumulenic equilibrium structure.[17]

Linear carbon chains possess axial symmetry (along the internuclear axis), and the electronic states are characterized in terms of the eigenfunctions, $e^{i\lambda\phi}$ (with $\lambda = 0, \pm1, \pm2, \ldots$), of the corresponding angular momentum operator. Therefore, the electronic states of C_{15}, C_{17}, C_{19}, and C_{21} chains studied here belong to both nondegenerate, ($\lambda = 0$) $^1\Sigma$, and doubly degenerate, ($\lambda = \pm1, \pm2, \ldots$) $^1\Pi$, $^1\Delta$, . . ., terms. About 12 excited electronic states are found to exist to within 4 eV energy in the vicinity of the optically bright, $^1\Sigma_u^+$, state of these carbon chains. The degeneracy of the Π, Δ, . . . states splits upon distortion (from equilibrium $D_{\infty h}$ configuration) along bending vibrational modes and gives rise to the Renner-Teller (RT) effect.[18] In addition, the RT split component electronic states may also undergo symmetry allowed coupling with the nondegenerate ($^1\Sigma$) or another RT split component state and can lead to a pseudo-Renner-Teller (PRT) type of interaction (equivalent to pseudo-Jahn-Teller interaction in nonlinear systems[19]) of the electronic states.[20] The $^1\Sigma_u^+$ electronic state is the optically brightest state in all the clusters studied here. Its oscillator strength scales linearly (cf. Fig. 1) with the cluster chain length. Several optically dark nondegenerate and degenerate electronic states appear to within 1.0 eV energy range in the vicinity of this $^1\Sigma_u^+$ state. Therefore, elucidation of the coupling mechanism of the latter state with its neighbors is important to unravel the details of intensity borrowing vis-à-vis experimental observations. Despite ample amount of experimental data, a rigorous theoretical study to understand them has been missing so far in the literature. The present effort is aimed to fulfill this task. We therefore first concentrate on analyzing the detailed coupling mechanism of Σ–Π electronic states of the mentioned carbon chains, through rigorous quantum chemistry calculations, and establish a coupling model in a diabatic electronic basis in order to perform dynamics studies (presented in Paper II[29]) to understand the experimental findings.

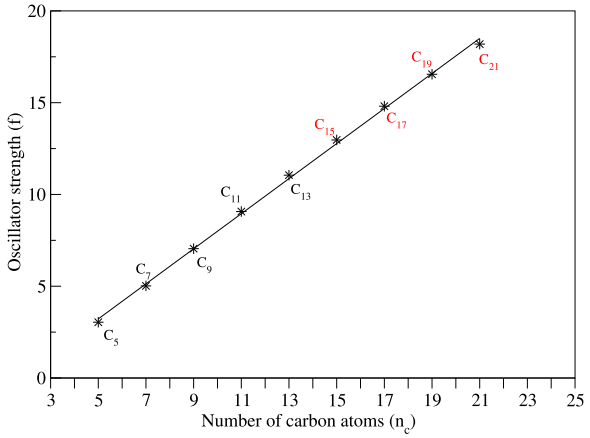

FIG. 1. Oscillator strength (f) of linear carbon chains with an odd number of carbon atoms as a function of the number of carbon atoms. The points indicated by the asterisks represent results obtained from *ab initio* quantum chemistry calculations employing the EOM-CCSD method with a cc-pVDZ basis set, and the solid line represents a linear fit to the *ab initio* data given by $f = -1.55 + 0.96\, n_c$.

II. ELECTRONIC STRUCTURE CALCULATIONS

The electronic ground state (S_0 $^1\Sigma_g^+$) of the carbon chains C_{2n+1} (n = 7–10) is taken as the reference state to investigate $^1\Sigma_u^+$ photoabsorption spectroscopy. The equilibrium geometry of the reference state is optimized by the Becke-3-parameter (exchange), Lee, Yang, and Parr (B3LYP) density functional method using the correlation consistent polarized valence double—ζ (cc-pVDZ) basis set of Dunning.[21] The Gaussian-09 suite of program[22] is used for the optimization calculations. The optimized equilibrium geometry yields an average C=C bond length of ~1.30 A^0 in agreement with the literature data.[23] Harmonic frequency (ω_k) of vibrational modes and their dimensionless normal displacement coordinates (Q_k) are calculated by diagonalizing the kinematic and force constant matrices of the reference equilibrium geometry at Q = 0. The frequencies are given in Table I.

Symmetry analysis reveals that the normal modes of linear carbon chains, C_{2n+1} (say, $2n + 1 = N$), decomposes into the following irreducible representations (IREPs) of the $D_{\infty h}$ symmetry point group as shown in the Appendix,

$$\Gamma = ((N-1)/2)\sigma_g^+ \oplus ((N-1)/2)\sigma_u^+ \oplus ((N-3)/2) \times \pi_g \oplus ((N-1)/2)\pi_u. \quad (1)$$

The analysis given in the Appendix also reveals that these linear molecules do not contain vibrations with higher angular momentum like δ and ϕ. The vertical excitation energies (VEEs) of the electronic states of C_{15}, C_{17}, C_{19}, and C_{21} are calculated along the dimensionless normal coordinates of all vibrational modes. The calculations are carried out using the EOM-CCSD method implemented in the MOLPRO suite of programs[24] and cc-pVDZ basis set. In MOLPRO, the calculations are performed in D_{2h} symmetry. The D_{2h}–$D_{\infty h}$ correlation table (given in the Appendix) is utilized to derive electronic terms and symmetry representation of vibrational modes. The VEEs calculated at the equilibrium geometry of the reference ground state of energetically low-lying (to within 4 eV relative to reference equilibrium energy) electronic states are given in Table II. Along with the VEEs, the oscillator strength values are also given in Table II. It can be seen that the $^1\Sigma_u^+$ is the only optically bright state in these carbon chains. The oscillator strength of this state for chains containing an odd number of C atoms from C_5 to C_{21} is plotted as a function of the chain length in Fig. 1. The asterisks in Fig. 1 represent the *ab initio* calculated values, and a linear regression fit to the *ab initio* data is shown by the line. The $\langle R \rangle^2$ value of the fit is 0.99. It can be seen from this figure that the oscillator strength increases linearly with increasing chain length. This is caused by an interplay of the transition probability and frequency of transition. The oscillator strength is directly proportional to the dipole transition moment. The large increase of the latter quantity compensates for the decrease in transition frequency for the clusters with increasing chain length. A linear relation of the quantities plotted in Fig. 1 seems to be fortuitous.

The VEEs are calculated over a range of normal displacement coordinates ($-5.00 \leq Q \leq 5.00$) of the vibrational modes. These

TABLE I. Symmetry representation and Harmonic frequency of the vibrational modes of C_{2n+1} (n = 7–10) in the $^1\Sigma_g^+$ electronic ground state.

C_{15}				C_{17}				C_{19}				C_{21}			
Symmetry	Mode	Frequency		Symmetry	Mode	Frequency		Symmetry	Mode	Frequency		Symmetry	Mode	Frequency	
	κ	eV	cm^{-1}		κ	eV	cm^{-1}		κ	eV	cm^{-1}		κ	eV	cm^{-1}
σ_g^+	ν_1	0.2780	2243	σ_g^+	ν_1	0.2798	2257	σ_g^+	ν_1	0.2799	2258	σ_g^+	ν_1	0.2790	2250
	ν_2	0.2748	2216		ν_2	0.2706	2182		ν_2	0.2721	2195		ν_2	0.2759	2225
	ν_3	0.2549	2055		ν_3	0.2648	2136		ν_3	0.2651	2138		ν_3	0.2615	2109
	ν_4	0.2175	1755		ν_4	0.2387	1925		ν_4	0.2503	2018		ν_4	0.2587	2087
	ν_5	0.1622	1308		ν_5	0.1954	1576		ν_5	0.2207	1780		ν_5	0.2376	1916
	ν_6	0.1014	817		ν_6	0.1452	1171		ν_6	0.1778	1434		ν_6	0.2026	1634
	ν_7	0.0349	281		ν_7	0.0902	727		ν_7	0.1313	1059		ν_7	0.1630	1314
σ_u^+	ν_8	0.2802	2260		ν_8	0.0308	249		ν_8	0.0811	654		ν_8	0.1198	967
	ν_9	0.2687	2167	σ_u^+	ν_9	0.2787	2248		ν_9	0.0276	222		ν_9	0.0737	594
	ν_{10}	0.2481	2001		ν_{10}	0.2743	2213	σ_u^+	ν_{10}	0.2782	2244		ν_{10}	0.0250	202
	ν_{11}	0.2386	1924		ν_{11}	0.2528	2039		ν_{11}	0.2754	2222	σ_u^+	ν_{11}	0.2792	2252
	ν_{12}	0.1903	1534		ν_{12}	0.2395	1932		ν_{12}	0.2623	2116		ν_{12}	0.2731	2202
	ν_{13}	0.1325	1069		ν_{13}	0.2191	1767		ν_{13}	0.2388	1926		ν_{13}	0.2686	2166
	ν_{14}	0.0688	555		ν_{14}	0.1709	1378		ν_{14}	0.2317	1869		ν_{14}	0.2488	2007
π_g	ν_{15}	0.0943	760		ν_{15}	0.1182	954		ν_{15}	0.1993	1608		ν_{15}	0.2258	1812
	ν_{16}	0.0735	593		ν_{16}	0.0610	492		ν_{16}	0.1550	1251		ν_{16}	0.2212	1784
	ν_{17}	0.0569	459	π_g	ν_{17}	0.0986	795		ν_{17}	0.1067	860		ν_{17}	0.1832	1478
	ν_{18}	0.0341	275		ν_{18}	0.0787	634		ν_{18}	0.0547	441		ν_{18}	0.1418	1143
	ν_{19}	0.0190	154		ν_{19}	0.0627	506	π_g	ν_{19}	0.1029	830		ν_{19}	0.0971	783
	ν_{20}	0.0064	51		ν_{21}	0.0403	325		ν_{20}	0.0834	673		ν_{20}	0.0496	400
π_u	ν_{21}	0.1063	857		ν_{21}	0.0289	233		ν_{21}	0.0674	543	π_g	ν_{21}	0.1074	866
	ν_{22}	0.0838	676		ν_{22}	0.0154	124		ν_{22}	0.0548	442		ν_{22}	0.0877	708
	ν_{23}	0.0648	523		ν_{23}	0.0051	41		ν_{23}	0.0362	292		ν_{23}	0.0717	578
	ν_{24}	0.0397	321	π_u	ν_{24}	0.1112	897		ν_{24}	0.0243	196		ν_{24}	0.0597	482
	ν_{25}	0.0268	216		ν_{25}	0.0884	713		ν_{25}	0.0126	101		ν_{25}	0.0411	331
	ν_{26}	0.0121	97		ν_{26}	0.0699	564		ν_{26}	0.0041	33		ν_{26}	0.0319	257
	ν_{27}	0.0023	19		ν_{27}	0.0557	449	π_u	ν_{27}	0.1163	938		ν_{27}	0.0205	166
					ν_{28}	0.0353	284		ν_{28}	0.0927	748		ν_{28}	0.0104	84
					ν_{29}	0.0220	177		ν_{29}	0.0747	602		ν_{29}	0.0034	27
					ν_{30}	0.0097	78		ν_{30}	0.0610	492	π_u	ν_{30}	0.1212	978
					ν_{31}	0.0019	15		ν_{31}	0.0407	328		ν_{31}	0.0968	781
									ν_{32}	0.0306	247		ν_{32}	0.0792	639
									ν_{33}	0.0181	146		ν_{33}	0.0654	528
									ν_{34}	0.0078	63		ν_{34}	0.0541	436
									ν_{35}	0.0015	12		ν_{35}	0.0369	298
													ν_{36}	0.0262	212
													ν_{37}	0.0152	122
													ν_{38}	0.0065	52
													ν_{39}	0.0012	10

energies plus the energy of the reference state define the adiabatic energies of the excited electronic states of the cluster chains. From Table II, it can be seen that the electronic states of the carbon chains studied here have Σ, Π, and Δ terms. All of them have a $^1\Sigma_g^+$ electronic ground term. The energy of the target $^1\Sigma_u^+$ state is lowered with increasing chain length. This state is energetically very close to its neighboring states (cf. Table II), and vibronic coupling is expected to play an important role in the nuclear dynamics on this state. The Π and Δ electronic states each are orbitally degenerate at the $D_{\infty h}$ symmetry configuration. This degeneracy is split

TABLE II. Vertical excitation energy (VEE in eV) and oscillator strength (*f*) of energetically low-lying excited singlet electronic states of neutral carbon clusters C_{15}, C_{17}, C_{19}, and C_{21}. The states marked with asterisk are considered in the dynamics study presented in Paper II. [29]

State	VEE	*f*	State	VEE	*f*
C_{15}			C_{17}		
$S_1\,^1\Delta_u$	0.670	0.00	$S_1\,^1\Delta_u$	0.552	0.00
$S_2\,^1\Sigma_u^-$	0.746	0.00	$S_2\,^1\Sigma_u^-$	0.632	0.00
$S_3\,^1\Sigma_g^-$	2.128	0.00	$S_3\,^1\Sigma_g^-$	1.864	0.00
$S_4\,^1\Delta_g$	2.143	0.00	$S_4\,^1\Delta_g$	1.869	0.00
$S_5^*\,^1\Pi_g$	3.108	0.00	$S_5^*\,^1\Sigma_u^+$	2.951	14.81
$S_6^*\,^1\Pi_u$	3.110	0.01	$S_6\,^1\Sigma_u^-$	3.060	0.00
$S_7^*\,^1\Sigma_u^+$	3.273	12.97	$S_7^*\,^1\Pi_u$	3.087	0.01
$S_8\,^1\Sigma_u^-$	3.432	0.00	$S_8^*\,^1\Pi_g$	3.089	0.00
$S_9\,^1\Sigma_g^-$	3.449	0.00	$S_9\,^1\Delta_u$	3.132	0.00
$S_{10}\,^1\Delta_g$	3.480	0.00	$S_{10}\,^1\Sigma_g^-$	3.163	0.00
$S_{11}\,^1\Delta_u$	3.515	0.00	$S_{11}\,^1\Delta_g$	3.199	0.00
$S_{12}^*\,^1\Sigma_g^+$	3.613	0.00	$S_{12}^*\,^1\Sigma_g^+$	3.346	0.00
C_{19}			C_{21}		
$S_1\,^1\Delta_u$	0.460	0.00	$S_1\,^1\Delta_u$	0.385	0.00
$S_2\,^1\Sigma_u^-$	0.541	0.00	$S_2\,^1\Sigma_u^-$	0.469	0.00
$S_3\,^1\Delta_g$	1.648	0.00	$S_3\,^1\Delta_g$	1.465	0.00
$S_4\,^1\Sigma_g^-$	1.652	0.00	$S_4\,^1\Sigma_g^-$	1.477	0.00
$S_5^*\,^1\Sigma_u^+$	2.678	16.55	$S_5^*\,^1\Sigma_u^+$	2.444	18.19
$S_6\,^1\Sigma_u^-$	2.753	0.00	$S_6\,^1\Sigma_u^-$	2.494	0.00
$S_7\,^1\Delta_u$	2.814	0.01	$S_7\,^1\Delta_u$	2.546	0.00
$S_8\,^1\Sigma_g^-$	2.928	0.00	$S_8\,^1\Sigma_g^-$	2.732	0.00
$S_9\,^1\Delta_g$	2.968	0.00	$S_9\,^1\Delta_g$	2.773	0.00
$S_{10}^*\,^1\Pi_g$	3.071	0.01	$S_{10}^*\,^1\Sigma_g^+$	2.939	0.00
$S_{11}^*\,^1\Pi_u$	3.072	0.00	$S_{11}^*\,^1\Pi_u$	3.060	0.01
$S_{12}^*\,^1\Sigma_g^+$	3.125	0.00	$S_{12}^*\,^1\Pi_g$	3.060	0.00

upon bending the linear chain and gives rise to the RT effect.[18] The RT split component states may undergo a PRT type of coupling with the nondegenerate $^1\Sigma_u^+$ state.[20] Using elementary symmetry rules, the following coupling scheme can be derived from the character table of the $D_{\infty h}$ symmetry point group.[25]

The first-order coupling between electronic states i and j through vibrational mode k is governed by the symmetry rule, $\Gamma_i \otimes \Gamma_k \otimes \Gamma_j \supset \sigma_g^+$.[25] The symbol Γ represents the IREPs. The symbol σ_g^+ is the IREP of totally symmetric vibrational mode of linear molecule of $D_{\infty h}$ symmetry. According to this rule, the latter vibrational modes are active within given electronic states ($i = j$). Now for the degenerate Π and Δ states, the symmetrized direct products transform according to $(\Pi_g)^2 = (\Pi_u)^2 = \sigma_g^+ + \delta_g$ and $(\Delta_g)^2 = (\Delta_u)^2 = \sigma_g^+ + \gamma_g$. While the totally symmetric σ_g^+ vibrational modes cannot lift orbital degeneracy, the modes of δ_g and γ_g symmetry can lift the same in the first-order of the Π and Δ states, respectively. The lack of vibrational modes of δ_g and γ_g symmetry in linear molecules (cf. the Appendix) makes the first-order RT coupling vanish in these states. However, $(\pi_g)^2 = (\pi_u)^2 \supset \delta_g$ and $(\pi_g)^4 = (\pi_u)^4 \supset \gamma_g$, therefore, the π_g and π_u modes can be RT active in the Π and Δ states in second-order and fourth-order, respectively. The RT split components of the Π and Δ states can undergo a PRT type of coupling according to

$$\Pi_g \otimes \Pi_u = \delta_u + \sigma_u^- + \sigma_u^+, \tag{2a}$$

$$\Pi_{g/u} \otimes \Delta_{g/u} = \pi_g + \phi_g, \tag{2b}$$

$$\Pi_{g/u} \otimes \Delta_{u/g} = \pi_u + \phi_u, \tag{2c}$$

$$\Delta_g \otimes \Delta_u = \gamma_u + \sigma_u^- + \sigma_u^+. \tag{2d}$$

The nondegenerate Σ state can undergo coupling with the neighboring Σ or Π states according to

$$\Sigma_u^+ \otimes \Sigma_g^+ = \sigma_u^+, \tag{3a}$$

$$\Sigma_u^+ \otimes \Pi_{g/u} = \pi_{u/g}, \tag{3b}$$

$$\Sigma_g^+ \otimes \Pi_{g/u} = \pi_{g/u}. \tag{3c}$$

It can be seen from Eqs. (3) that direct coupling of the Σ_u^+ state in first-order with $\Pi_{g/u}$ and also the Σ_g^+ state is possible through $\pi_{g/u}$ and σ_u^+ vibrational modes. However, a direct coupling of the Σ_u^+ state and the $\Delta_{g/u}$ state in first-order is not possible as it requires vibrational modes of δ symmetry. Therefore, in the following, the coupling between the Σ_u^+ state with its neighboring $\Pi_{g/u}$ and Σ_g^+ state is examined in detail.

III. THE VIBRONIC HAMILTONIAN

It can be seen from Table II that in the immediate neighborhood of $^1\Sigma_u^+$ states, there are many states of Σ, Π, and Δ symmetry. Consideration of all states listed in Table II in the dynamics (treated in Paper II[29]) is computationally not possible. We therefore selected the states marked with an asterisk in Table II and developed a vibronic Hamiltonian in the following. It can be seen from Table II that in addition to the $^1\Sigma_u^+$ state, the $^1\Pi_g$, $^1\Pi_u$, and $^1\Sigma_g^+$ state (one each) is considered. These states are energetically closest to the $^1\Sigma_u^+$ state. With the aid of the symmetry rules discussed in Sec. II and standard vibronic coupling theory,[26] the following vibronic Hamiltonian is derived in a diabatic electronic basis:

$$\mathcal{H} = \mathcal{H}_0 \mathbf{1}_6 + \Delta\mathcal{H}, \tag{4}$$

where $\mathcal{H}_0 = \mathcal{T}_N + \mathcal{V}_0$, with

$$\mathcal{T}_N = -\frac{1}{2}\sum_{k \in \sigma_g^+,\,\sigma_u^+} \omega_k \frac{\partial^2}{\partial Q_k^2} - \frac{1}{2}\sum_{k \in \pi_g,\,\pi_u} \omega_k \left(\frac{\partial^2}{\partial Q_{kx}^2} + \frac{\partial^2}{\partial Q_{ky}^2} \right)$$

and

$$\mathcal{V}_0 = \frac{1}{2}\sum_{k \in \sigma_g^+,\,\sigma_u^+} \omega_k Q_k^2 + \frac{1}{2}\sum_{k \in \pi_g,\,\pi_u} \omega_k \left(Q_{kx}^2 + Q_{ky}^2 \right),$$

is the unperturbed harmonic Hamiltonian of the reference electronic ground state. $\mathbf{1}_6$ is a 6×6 unit matrix. The components of doubly degenerate vibrational mode and electronic state are labeled with x and y, respectively. The quantity, $\Delta\mathcal{H}$, defines the change in

TABLE III. Off-diagonal terms of the Hamiltonian [Eq. (5)] representing RT and PRT coupling.

	$H_1(^1\Sigma_u^+)$	$H_2(^1\Pi_{gx})$	$H_3(^1\Pi_{gy})$	$H_4(^1\Pi_{ux})$	$H_5(^1\Pi_{uy})$	$H_6(^1\Sigma_g^+g)$
$H_1(^1\Sigma_u^+)$		$\sum_{k\in\pi_u}\lambda_k^{1,2}Q_{kx}$	$\sum_{k\in\pi_u}\lambda_k^{1,3}Q_{ky}$	$\sum_{k\in\pi_g}\lambda_k^{1,4}Q_{kx}$	$\sum_{k\in\pi_g}\lambda_k^{1,5}Q_{ky}$	$\sum_{k\in\sigma_u^+}\lambda_k^{1,6}Q_k$
$H_2(^1\Pi_{gx})$			$\sum_{k\in\pi_g,\pi_u}2\eta_k^{(2,3)}(Q_{kx}Q_{ky})+$ $\sum_{k\in\pi_g,\pi_u}2\beta_k^{(2,3)}(Q_{kx}^3Q_{ky}+Q_{kx}Q_{ky}^3)$	$\sum_{k\in\sigma_u^+}\lambda_k^{2,4}Q_k$	...	$\sum_{k\in\pi_g}\lambda_k^{2,6}Q_{kx}$
$H_3(^1\Pi_{gy})$				...	$\sum_{k\in\sigma_u^+}\lambda_k^{3,5}Q_k$	$\sum_{k\in\pi_g}\lambda_k^{3,6}Q_{ky}$
$H_4(^1\Pi_{ux})$					$\sum_{k\in\pi_g,\pi_u}2\eta_k^{(4,5)}(Q_{kx}Q_{ky})+$ $\sum_{k\in\pi_g,\pi_u}2\beta_k^{(4,5)}(Q_{kx}^3Q_{ky}+Q_{kx}Q_{ky}^3)$	$\sum_{k\in\pi_u}\lambda_k^{4,6}Q_{kx}$
$H_5(^1\Pi_{uy})$		*h.c.*				$\sum_{k\in\pi_u}\lambda_k^{5,6}Q_{ky}$
$H_6(^1\Sigma_g^+)$						

electronic energy upon excitation. This is a 6 × 6 matrix Hamiltonian in a diabatic electronic basis that can be symbolically expressed as

$$\Delta\mathcal{H}=\begin{bmatrix} H_1 & H_{12} & H_{13} & H_{14} & H_{15} & H_{16}\\ & H_2 & H_{23} & H_{24} & H_{25} & H_{26}\\ & & H_3 & H_{34} & H_{35} & H_{36}\\ & & & H_4 & H_{45} & H_{46}\\ & h.c. & & & H_5 & H_{56}\\ & & & & & H_6 \end{bmatrix}. \tag{5}$$

In Eq. (5), the states identified with the index 1–6 refer to $^1\Sigma_u^+$, $^1\Pi_{gx}$, $^1\Pi_{gy}$, $^1\Pi_{ux}$, $^1\Pi_{uy}$, and $^1\Sigma_g^+$, respectively. The diagonal elements of this Hamiltonian matrix for degenerate electronic states $^1\Pi_{gx}$, $^1\Pi_{gy}$, $^1\Pi_{ux}$, and $^1\Pi_{uy}$ are expanded in a Taylor series around the reference equilibrium configuration in the following way:

$$\begin{aligned}\mathcal{H}_i=\mathcal{E}_i^0&+\sum_{k\,\in\,\sigma_g^+}\kappa_k^iQ_k+\sum_{k\,\in\,\sigma_g^+,\,\sigma_u^+}\gamma_k^iQ_k^2+\sum_{k\,\in\,\pi_g,\,\pi_u}\gamma_k^i(Q_{kx}^2+Q_{ky}^2)\\&+\sum_{k\,\in\,\pi_g,\,\pi_u}\rho_k^i(Q_{kx}^2+Q_{ky}^2)^2\pm\sum_{k\,\in\,\pi_g,\,\pi_u}\eta_k^{i,j}(Q_{kx}^2-Q_{ky}^2)\\&\pm\sum_{k\,\in\,\pi_g,\,\pi_u}\beta_k^{i,j}(Q_{kx}^4-Q_{ky}^4);\ i=2-5.\end{aligned} \tag{6}$$

The last three terms in Eq. (6) drop out in the expansion of $\mathcal{H}_i$ (i = 1, 6) for the nondegenerate, $^1\Sigma_u^+$ and $^1\Sigma_g^+$, electronic states.

In the above, $\mathcal{E}_i^0$ defines the VEE of the ith electronic state. The quantities κ_k^i, γ_k^i, and ρ_k^i define the first-order, second-order, and fourth-order intrastate coupling parameters along vibrational mode k of the ith electronic state, respectively. The + and − sign of the last two terms of Eq. (6) applies to the x and y component of the degenerate Π state and degenerate π vibrational modes. The quantities, $\eta_k^{i,j}$ and $\beta_k^{i,j}$, are the quadratic and quartic RT coupling parameters within the Π states, respectively. The various off-diagonal terms of the Hamiltonian of Eq. (5) representing RT and PRT couplings are given in Table III.

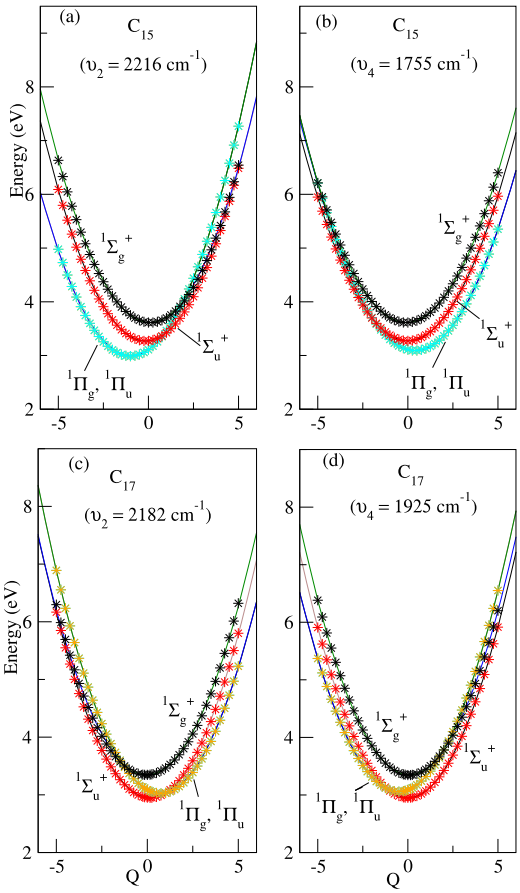

FIG. 2. Adiabatic potential energies of the low-lying excited singlet electronic states, $^1\Sigma_u^+$, $^1\Pi_g$, $^1\Pi_u$, and $^1\Sigma_g^+$ of C_{15} [(a) and (b)] and C_{17} [(c) and (d)] along the normal coordinate of totally symmetric σ_g^+ vibrational modes given in each panel. The potential energies obtained from the present vibronic model are shown by the solid lines, and the computed *ab initio* energies are shown by the asterisk.

In Table III, $\lambda_k^{i,j}$ defines the linear PRT coupling parameter between states i and j along the vibrational mode k. The quadratic and quartic RT coupling parameters within the Π states are given by $\eta_k^{i,j}$ and $\beta_k^{i,j}$ along the vibrational mode k. All the coupling parameters defined above are estimated from the calculated adiabatic electronic energies along a given vibrational mode. Nonlinear least squares fit of the adiabatic energies to the adiabatic form of the diabatic Hamiltonian of Eq. (5) along each vibrational mode is carried out for this purpose. The complete list of parameters for all four clusters is given in Tables S1–S8 of the supplementary material. A close look at the parameters given in these tables reveals that the lowest frequency, σ_g^+ vibrational mode (ν_7 in C_{15}, ν_8 in C_{17}, ν_9 in C_{19}, and ν_{10} in C_{21}) possesses large excitation strength in the $^1\Sigma_u^+$ state.

The excitation strength of the symmetric vibrational modes is nearly the same in both the $^1\Pi_g$ and $^1\Pi_u$ states of all four carbon chains. It can be seen from Table II that the latter two states are quasidegenerate at the vertical configurations of all four carbon chains. A similar value of κ and γ of these states is again discussed later in the text in relation to the topography of their potential energy surfaces along σ_g^+ vibrational modes.

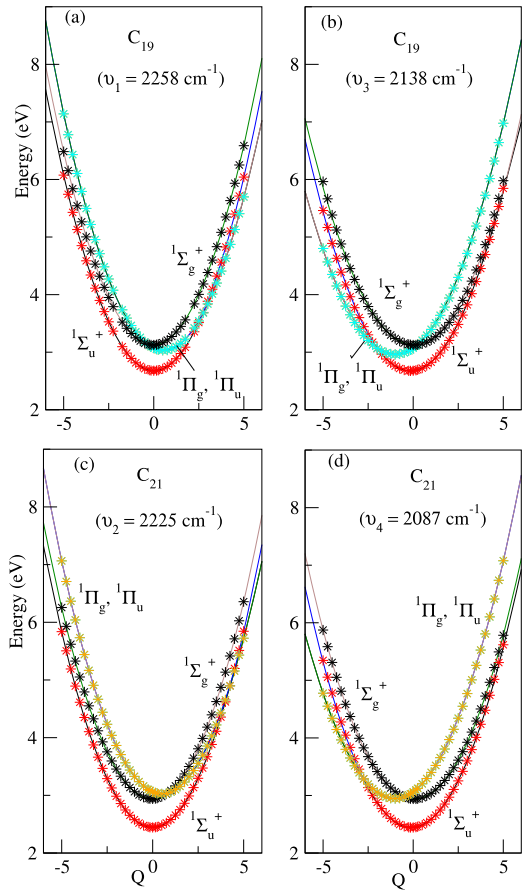

FIG. 3. Same as in Fig. 2, for $^1\Sigma_u^+$, $^1\Pi_g$, $^1\Pi_u$, and $^1\Sigma_g^+$ electronic states of C_{19} [(a) and (b)] and C_{21} [(c) and (d)].

IV. RESULTS AND DISCUSSION

A. Adiabatic potential energy surfaces

Here, we examine and discuss on the topography of the adiabatic PESs of six (including degeneracy) excited singlet electronic states (as mentioned above) obtained by diagonalizing the diabatic electronic Hamiltonian constructed above. One dimensional cuts of the potential energy hypersurfaces of C_{2n+1} (where n = 7–10) are plotted along the normal displacement coordinate of the totally symmetric (σ_g^+) and RT active (π_g and π_u) vibrational modes keeping others at their equilibrium positions at **Q** = 0 in each case. These plots are shown in Figs. 2–6. In each figure, the solid curves represent the adiabatic potential energy obtained from the diabatic model developed in Sec. II and the corresponding parameters given in Tables S1–S8 of the supplementary material. The points superimposed on the curves are obtained from *ab initio* quantum chemistry calculations discussed in Sec. II. It can be seen from Figs. 2–6

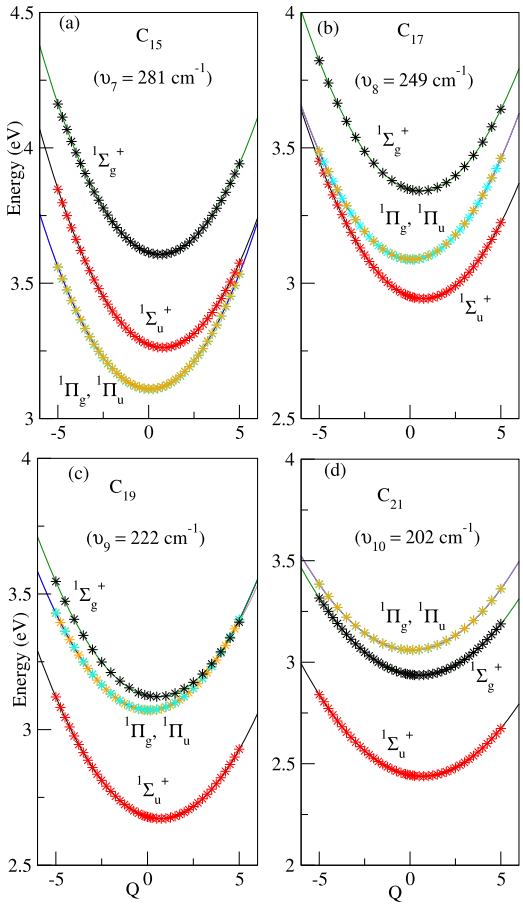

FIG. 4. Adiabatic potential energies of the low-lying excited singlet electronic states, $^1\Sigma_u^+$, $^1\Pi_g$, $^1\Pi_u$, and $^1\Sigma_g^+$ of C_{15} (a), C_{17} (b), C_{19} (c), and C_{21} (d), along the normal coordinate of lowest frequency totally symmetric σ_g^+ vibrational mode. The potential energies obtained from the present vibronic model are shown by the solid lines, and the computed *ab initio* energies are shown by the asterisk.

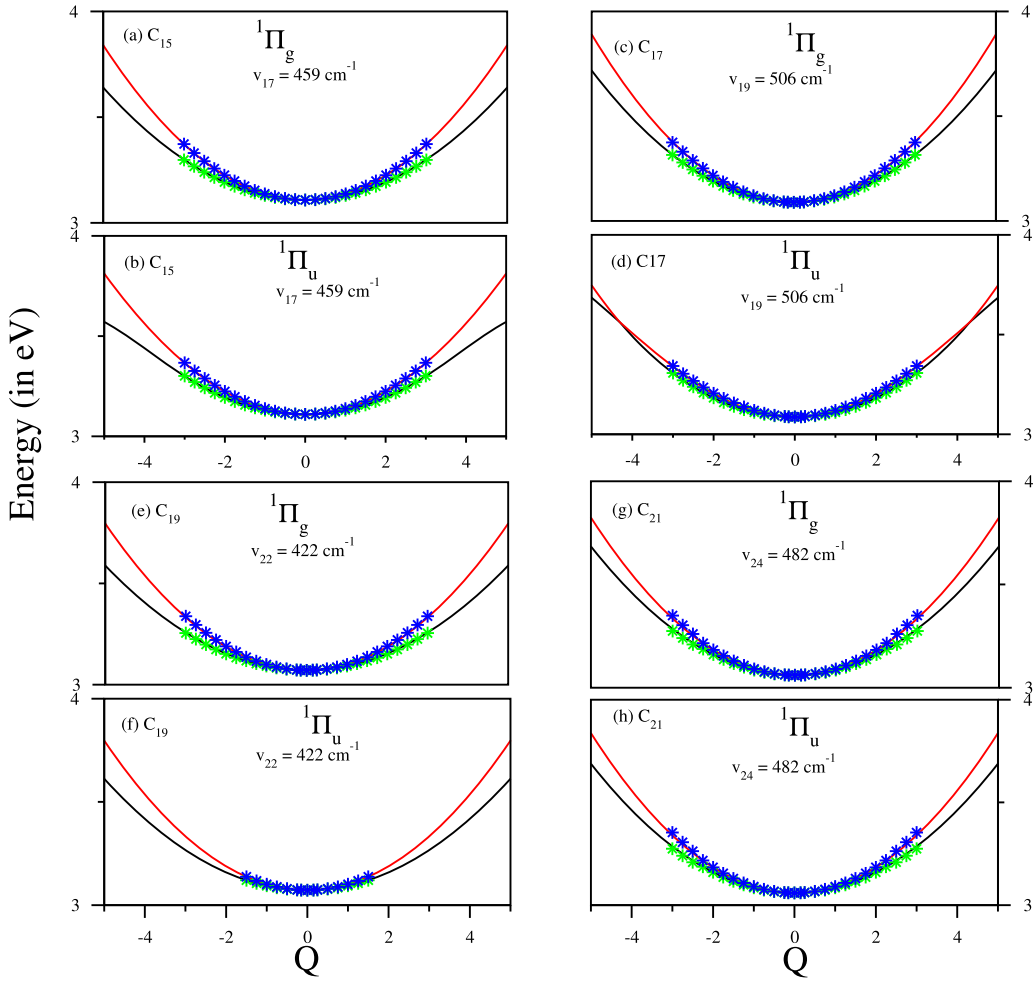

FIG. 5. Adiabatic potential energies of the low-lying excited singlet degenerate electronic states, $^1\Pi_g$ and $^1\Pi_u$ of C_{15} [(a) and (b)], C_{17} [(c) and (d)], C_{19} [(e) and (f)], and C_{21} [(g) and (h)], along the normal coordinate of RT active π_g vibrational modes. The potential energies obtained from the present vibronic model are shown by the solid lines, and the computed *ab initio* energies are shown by the asterisk.

that the calculated *ab initio* energies are very well reproduced by the constructed model. We note that a few representative potential energy curves are only shown in the above figures in order to facilitate the understanding of the dynamical outcomes presented in Paper II.[29]

It can be seen from Figs. 2–4 that the potential energy curves of $^1\Pi_g$ and $^1\Pi_u$ electronic states of all four carbon chains are almost degenerate. The energy curves appear exactly superimposable, and their slopes and curvatures at Q = 0 (equilibrium geometry of the reference ground state) remain identical in all four carbon chains. This yields identical values of κ and γ along σ_g^+ modes in both $^1\Pi_g$ and $^1\Pi_u$ states as given in Tables S1, S3, S5, and S7. Low-energy curve crossing of the $^1\Sigma_u^+$ state with $^1\Pi_g$ and $^1\Pi_u$ states can be seen to exist in all four carbon chains (cf. Figs. 2–4). The $^1\Sigma_g^+$ state also appears to have low-energy curve crossings with the $^1\Pi_g$ and $^1\Pi_u$ states. Unlike in the case in Figs. 2 and 3, the potential energy curves plotted along the lowest frequency σ_g^+ vibrational mode in Fig. 4 reveal that the $^1\Sigma_u^+$ state is energetically well separated from the rest of the states at its equilibrium minimum. This mode has the largest excitation strength in the $^1\Sigma_u^+$ state in all four carbon chains (cf. Tables S1, S3, S5, and S8) which is obvious from a considerable shift of the minimum of the potential energy curves (from the reference equilibrium minimum at Q = 0) of the $^1\Sigma_u^+$ state along this mode in Fig. 4. The various curve crossings seen in the potential energy curves in Figs. 2–4 would develop into conical intersections in multidimension. An analysis of the stationary points, viz., the equilibrium minimum of a state and the energetic minimum of the seam of various conical intersections, is carried out and presented later in this section. The implication of these stationary points on the nuclear dynamics is discussed in Paper II. [29]

Representative potential energy functions along the coordinate of the RT active π_g and π_u vibrational modes are shown in Figs. 5

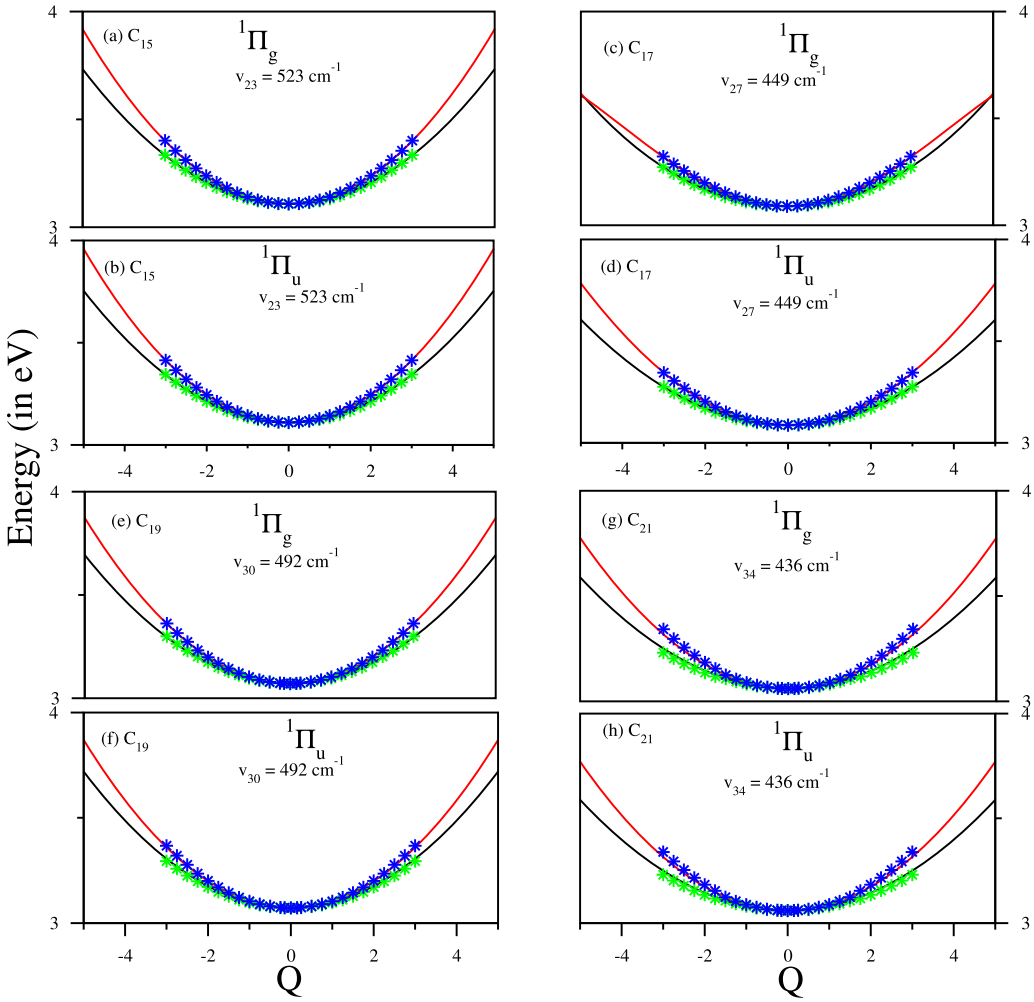

FIG. 6. Same as in Fig. 5, along the RT active π_u vibrational modes of C_{15} [(a) and (b)], C_{17} [(c) and (d)], C_{19} [(e) and (f)], and C_{21} [(g) and (h)].

and 6, respectively. It can be seen from these plots that the RT splitting of degeneracy of both the Π_g and Π_u electronic states of all four carbon chains is quite small. This is in accordance with the small value of the second-order RT coupling parameters (in the order of $\sim 10^{-3}$ or less) given in Tables S1, S3, S5, and S7 for C_{15}, C_{17}, C_{19}, and C_{21}, respectively.

As stated above, the curve crossings present in Figs. 2–4 form the seam of various conical intersections in multidimension. The energetic minimum of the seam of these CIs and the minimum of the upper adiabatic electronic states are estimated with a quadratic coupling model. A constrained optimization with the Lagrange multiplier as implemented in Mathematica[27] is used to estimate these energetic minima. The resulting data are given in Table IV. The diagonal entries in this table represent the energy at the equilibrium minimum of a state. However, the off-diagonal entries represent the minimum of the energy along the seam of CIs. The impact of these stationary points on the nuclear dynamics of all four carbon chains is discussed in Paper II. [29]

In the case of C_{15}, the $^1\Sigma_u^+$ electronic state is vertically above the $^1\Pi_g$ and $^1\Pi_u$ states and below the $^1\Sigma_g^+$ state (cf. Table II). The degenerate $^1\Pi_g$ and $^1\Pi_u$ states undergo curve crossing with the $^1\Sigma_u^+$ state along the normal coordinate of vibrational modes of σ_g^+ symmetry (cf. Fig. 2). It can be seen that the $^1\Pi_g$ and $^1\Pi_u$ electronic states are not only quasidegenerate at their equilibrium minimum but over a wide range of displaced nuclear configuration [cf. Figs. 2(a) and 2(b)]. Vertically, these states are separated by only ~0.002 eV (cf. Table II). The minimum of $^1\Pi_g$–$^1\Pi_u$ intersection occurs ~1.82 eV above the minimum of the $^1\Pi_u$ electronic state (cf. Table IV). From the data given in Table S2, it can be seen that the interstate coupling between these states is moderately strong along the antisymmetric stretch, ν_{10} (2001 cm^{-1}) and ν_{11} (1924 cm^{-1}) vibrational modes of σ_u^+ symmetry. Similarly, the minimum of the $^1\Sigma_u^+$ state

TABLE IV. Estimated equilibrium minimum (diagonal entries) and minimum of the seam of various intersections (off-diagonal entries) of the electronic states of C_{15}, C_{17}, C_{19}, and C_{21} within a quadratic coupling model. All quantities are given in eV unit.

			C_{15}					C_{17}	
	$^1\Sigma_u^+$	$^1\Pi_g$	$^1\Pi_u$	$^1\Sigma_g^+$		$^1\Sigma_u^+$	$^1\Pi_g$	$^1\Pi_u$	$^1\Sigma_g^+$
$^1\Sigma_u^+$	3.26	3.30	3.30	5.97	$^1\Sigma_u^+$	2.94	2.96	2.96	6.21
$^1\Pi_g$	...	2.91	4.73	3.77	$^1\Pi_g$	...	2.88	3.99	3.37
$^1\Pi_u$	...	...	2.91	3.77	$^1\Pi_u$	...	...	2.87	3.37
$^1\Sigma_g^+$	...	...	...	3.60	$^1\Sigma_g^+$	...	...	...	3.34
			C_{19}					C_{21}	
	$^1\Sigma_u^+$	$^1\Pi_g$	$^1\Pi_u$	$^1\Sigma_g^+$		$^1\Sigma_u^+$	$^1\Pi_g$	$^1\Pi_u$	$^1\Sigma_g^+$
$^1\Sigma_u^+$	2.67	2.84	2.84	5.72	$^1\Sigma_u^+$	2.44	2.85	2.85	6.73
$^1\Pi_g$	...	2.84	3.27	3.12	$^1\Pi_g$	...	2.82	3.12	2.96
$^1\Pi_u$	...	...	2.84	3.12	$^1\Pi_u$	...	...	2.84	2.96
$^1\Sigma_g^+$	...	...	...	3.12	$^1\Sigma_g^+$	...	...	...	2.93

is only ~0.04 eV lower in energy than the minimum of the $^1\Sigma_u^+$–$^1\Pi_g$ and $^1\Sigma_u^+$–$^1\Pi_u$ PRT intersection minimum (cf. Table IV). Strong interstate coupling between these states is caused by the π_u and π_g vibrational modes (cf. Table S2). Hence, it is expected that the absorption band of $^1\Pi_g$, $^1\Pi_u$, and $^1\Sigma_u^+$ states will be perturbed significantly by the $^1\Pi_g$–$^1\Sigma_u^+$ and $^1\Pi_u$–$^1\Sigma_u^+$ interstate couplings. However, the minimum of $^1\Pi_g$–$^1\Sigma_g^+$ and $^1\Pi_u$–$^1\Sigma_g^+$ CIs occurs ~0.12 eV above the minimum of the $^1\Sigma_g^+$ electronic state (cf. Table IV), the coupling between these states is weak (cf. Table S2). The $^1\Sigma_u^+$–$^1\Sigma_g^+$ intersection minimum occurs at much higher energy ~2.7 eV above the $^1\Sigma_u^+$ minimum (cf. Table IV). This separation is relatively large when compared to the remaining energetic locations discussed above. It can be seen from Figs. 2(a) and 2(b) that along the coordinates of ν_2 (2216 cm^{-1}) and ν_4 (1755 cm^{-1}) symmetric stretch vibrational modes, low-energy crossings among $^1\Sigma_u^+$–$^1\Pi_g$–$^1\Pi_u$–$^1\Sigma_g^+$ states of C_{15} appear.

In the case of C_{17}, the optically bright $^1\Sigma_u^+$ electronic state is vertically below the $^1\Pi_g$, $^1\Pi_u$, and $^1\Sigma_g^+$ states (cf. Table II). The minimum of this state occurs very close to the minimum of its seam of intersections with the $^1\Pi_g$ and $^1\Pi_u$ states (cf. Table IV). The $^1\Pi_g$ and $^1\Pi_u$ electronic states are quasidegenerate and have approximately the same energy at equilibrium minimum [cf. Figs. 2(c) and 2(d) and Table IV]. From Table S4, it can be seen that interstate coupling between these states is moderately strong along the antisymmetric stretch, ν_{12} (1932 cm^{-1}) vibrational mode of σ_u^+ symmetry. The $^1\Sigma_u^+$–$^1\Pi_g$ and $^1\Sigma_u^+$–$^1\Pi_u$ intersection minimum occurs ~0.08 eV and ~0.09 eV, respectively, above the minimum of the $^1\Pi_g$ and $^1\Pi_u$ states. Interstate coupling between $^1\Sigma_u^+$–$^1\Pi_g$ and $^1\Sigma_u^+$–$^1\Pi_u$ states is very strong along the low frequency π_u and π_g bending vibrational modes (cf. Table S4). Like in the case of C_{15}, low-energy crossings of $^1\Sigma_u^+$–$^1\Pi_g$–$^1\Pi_u$–$^1\Sigma_g^+$ electronic states along the symmetric stretch vibrational modes, ν_2 (2182 cm^{-1}) and ν_4 (1925 cm^{-1}) [cf. Figs. 2(c) and 2(d)], can be found for C_{17} also. The $^1\Sigma_u^+$–$^1\Sigma_g^+$ intersection minimum occurs ~3.0 eV above the $^1\Sigma_u^+$ minimum.

The $^1\Sigma_u^+$ electronic state is vertically below the $^1\Pi_g$, $^1\Pi_u$, and $^1\Sigma_g^+$ electronic states (cf. Table II) in the case of C_{19} chain. Again the $^1\Pi_g$ and $^1\Pi_u$ electronic states are quasidegenerate with nearly the same energy at equilibrium minimum in this case also [cf. Figs. 3(a) and 3(b) and Table IV]. The minimum of $^1\Pi_g$–$^1\Pi_u$ intersections is ~0.43 eV above the minimum of the $^1\Pi_u$ electronic state, and these states are strongly coupled along the antisymmetric stretch vibrational modes, ν_{11} (2222 cm^{-1}), ν_{14} (1869 cm^{-1}), and ν_{16} (1251 cm^{-1}) (cf. Table S6) of σ_u^+ symmetry. The minimum of $^1\Sigma_u^+$–$^1\Pi_g$ and $^1\Sigma_u^+$–$^1\Pi_u$ intersections is energetically very close to the minimum of the $^1\Pi_g$ and $^1\Pi_u$ states. These intersections are just ~0.17 eV above the minimum of the $^1\Sigma_u^+$ state. The interstate coupling between these states is strong along the low-frequency π_g and π_u vibrational modes (cf. Table S6). The minimum of $^1\Sigma_u^+$–$^1\Sigma_g^+$ conical intersections occurs at much higher energy, ~2.6 eV above the equilibrium minimum of the $^1\Sigma_g^+$ state. These states are fairly strongly coupled by the antisymmetric stretch, ν_{14} (1869 cm^{-1}) vibrational mode of σ_u^+ symmetry.

Like in the case of C_{17} and C_{19}, the $^1\Sigma_u^+$ electronic state is vertically below the $^1\Pi_g$, $^1\Pi_u$, and $^1\Sigma_g^+$ states in C_{21} also (cf. Table II). Quasidegeneracy of the $^1\Pi_g$ and $^1\Pi_u$ electronic states is found in this case also [cf. Table IV and Figs. 3(c) and 3(d)]. The minimum of the $^1\Pi_u$–$^1\Pi_g$ intersections occurs ~0.30 eV above the minimum of the $^1\Pi_g$ electronic state. These states are strongly coupled along the antisymmetric stretch, ν_{13} (2166 cm^{-1}), ν_{15} (1821 cm^{-1}), and ν_{16} (1784 cm^{-1}) (cf. Table S8) vibrational modes of σ_u^+ symmetry. The $^1\Sigma_u^+$ – $^1\Pi_g$ and $^1\Sigma_u^+$ – $^1\Pi_u$ intersection minima are close to the minimum of the $^1\Pi_g$ and $^1\Pi_u$ state, with an energy gap of ~0.01 and ~0.03 eV, respectively. These intersections occur ~0.41 eV above the minimum of the $^1\Sigma_u^+$ state (cf. Table IV). The interstate coupling between these states is strong along the low frequency π_g and π_u bending vibrational modes. The $^1\Sigma_u^+$–$^1\Sigma_g^+$ conical intersection minimum occurs at much higher energy, ~3.8 eV above the minimum of the $^1\Sigma_g^+$ state. The coupling is weak between these states (cf. Table S8).

The above discussion reveals that the energetic minimum of the seam of various CIs generally moves to higher energy relative to the minimum of the $^1\Sigma_u^+$ electronic state with an increase in length of the carbon chain which appears to have a quite different impact on their nuclear dynamics (cf. Paper II[29]).

V. SUMMARIZING REMARKS

The structure and energetics of the six (including degeneracy) energetically close lying electronic states (viz., $^1\Sigma_u^+$, $^1\Pi_g$, $^1\Pi_u$, and $^1\Sigma_g^+$) of neutral carbon chains, C_{2n+1} (n = 7–10), have been investigated here as a prerequisite for the dynamics study (presented in Paper II[29]) to examine their photoabsorption spectrum. The electronic energies are calculated by the EOM-CCSD method along the normal coordinate of the vibrational modes. The linear carbon chains, C_{2n+1} (n = 7–10), studied here have a $^1\Sigma_g^+$ ground electronic term. For all of them, it is seen that the $^1\Sigma_u^+$ electronic state is optically bright with large oscillator strength and the latter scales linearly with the chain length.

A model diabatic Hamiltonian is constructed in terms of dimensionless normal coordinates and considering six electronic states which are in the immediate vicinity of the $^1\Sigma_u^+$ state to study the nuclear dynamics. The Hamiltonian is parameterized by carrying out adiabatic *ab initio* electronic energy calculations. The topography of the potential energy surfaces along normal coordinates of vibrational modes is examined in detail. It is found that the RT splitting of the degenerate Π state is small in all four carbon chains. However, significant PRT coupling among $^1\Sigma_u^+$–$^1\Pi_g$–$^1\Pi_u$–$^1\Sigma_g^+$ electronic states is found. The location of the energetic minimum of the seam of various conical intersections relative to the equilibrium minimum of a state is calculated. The impact of the latter energetics of potential energy surfaces on the nuclear dynamics of the four carbon chains, C_{2n+1} (n = 7–10), is discussed in Paper II. [29]

SUPPLEMENTARY MATERIAL

See supplementary material for the coupling parameters of the electronic Hamiltonian [cf. Eq. (6)] and Table III for C_{15} (Tables S1 and S2), C_{17} (Tables S3 and S4), C_{19} (Tables S5 and S6), and C_{21} (Tables S7 and S8).

ACKNOWLEDGMENTS

This study was in part financially supported by a research grant from the Department of Science and Technology, New Delhi (Grant No. EMR/2017/004592). S.M. also acknowledges the University Grants Commission, New Delhi, for the UGC-BSR Mid Career award. The authors thank Arun Kumar Kanakati and Mamilwar Rani for the help in preparation of the manuscript.

APPENDIX: SYMMETRY REPRESENTATION OF VIBRATIONAL MODES OF LINEAR CARBON CHAIN WITH N CARBON ATOMS

The carbon chains studied in this paper possess equilibrium geometry of $D_{\infty h}$ point group symmetry. The highest Abelian point group that correlates with $D_{\infty h}$ is D_{2h}. The correlation table in terms of the electronic states and vibrational modes is given below. The molecule is considered to be in the Y-Z plane, and the X axis is perpendicular to the molecular plane, as sketched in Fig. 7.

In the following, a general equation is derived with the aid of the orthogonality theorem for the symmetry representation of a linear molecule containing N atoms belonging to the $D_{\infty h}$ equilibrium symmetry point group.

The correlation table for the electronic states and vibrational modes in the $D_{\infty h}$–D_{2h} symmetry groups reads[28]

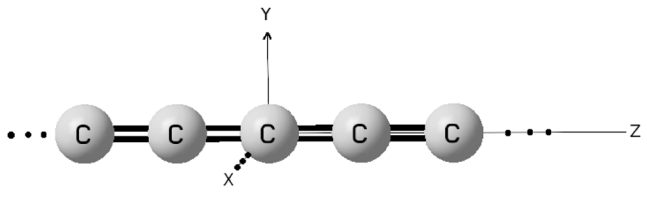

FIG. 7. A schematic representation of linear carbon chains in the Y-Z plane.

$D_{\infty h}$	D_{2h}	$D_{\infty h}$	D_{2h}
Electronic term	(IREPs)	Vibrational mode	(IREPs)
Σ_g^+	A_g	σ_g^+	a_g
Σ_g^-	B_{1g}	σ_g^-	b_{1g}
Σ_u^+	B_{1u}	σ_u^+	b_{1u}
Σ_u^-	A_u	σ_u^-	a_u
Π_g	$B_{2g} + B_{3g}$	π_g	$b_{2g} + b_{3g}$
Π_u	$B_{2u} + B_{3u}$	π_u	$b_{2u} + b_{3u}$
Δ_g	$A_g + B_{1g}$	δ_g	$a_g + b_{1g}$
Δ_u	$A_u + B_{1u}$	δ_u	$a_u + b_{1u}$

The reducible representation of N atom carbon chain in the D_{2h} symmetry group is given by

D_{2h}	E	$C_2(z)$	$C_2(y)$	$C_2(x)$	i	$\sigma(xy)$	$\sigma(xz)$	$\sigma(yz)$
Γ_{red}	3N	−N	−1	−1	−3	1	N	N

Upon decomposition to component irreducible representation of the D_{2h} symmetry point group, the total number of IREPs in Γ_{red} is given by

$$\Gamma_{total} = \frac{(N-1)}{2}a_g + \frac{(N+1)}{2}b_{1u} + \frac{(N-1)}{2}(b_{2g}+b_{3g}) + \frac{(N+1)}{2}(b_{2u}+b_{3u}). \quad \text{(A1)}$$

Using the D_{2h}-$D_{\infty h}$ (*vide supra*) correlation table given above the above equation (A1) in the symmetry representation of the $D_{\infty h}$ point group reads

$$\Gamma_{total} = \frac{(N-1)}{2}\sigma_g^+ + \frac{(N+1)}{2}\sigma_u^+ + \frac{(N-1)}{2}\pi_g + \frac{(N+1)}{2}\pi_u. \quad \text{(A2)}$$

The two rotational degrees of freedom of the N atom carbon chain transform as (b_{1g} drops out in $D_{\infty h}$ as it rotates along the molecular axis)

$$\Gamma_{rotational} = 1b_{2g} + 1b_{3g} + 1b_{1g}\ (in\ D_{2h}) = 1\pi_g + 0\ (in\ D_{\infty h}). \quad \text{(A3)}$$

The three translational degrees of freedom transform as

$$\Gamma_{translational} = 1b_{2u} + 1b_{3u} + 1b_{1u}\ (in\ D_{2h}) = 1\pi_u + 1\sigma_u^+\ (in\ D_{\infty h}). \quad \text{(A4)}$$

Now, the IREPs of the vibrational modes of the N atom carbon chains read

$$\begin{aligned}\Gamma_{vibrational} &= \Gamma_{total} - \Gamma_{rotational} - \Gamma_{translational}\\ &= \frac{(N-1)}{2}a_g + \frac{(N-1)}{2}b_{1u} + \frac{(N-3)}{2}(b_{2g}+b_{3g})\\ &\quad + \frac{(N-1)}{2}(b_{2u}+b_{3u})\ (in\ \mathrm{D}_{2h})\\ &= \frac{(N-1)}{2}\sigma_g^+ + \frac{(N-1)}{2}\sigma_u^+ + \frac{(N-3)}{2}\pi_g\\ &\quad + \frac{(N-1)}{2}\pi_u\ (in\ \mathrm{D}_{\infty h}). \qquad \text{(A5)}\end{aligned}$$

The above analysis shows that linear molecules with $D_{\infty h}$ symmetry point group do not contain modes with vibrational angular momentum quantum number >±1. Therefore, the electronic Π and higher angular momentum states are not RT active in the first-order in accordance with the selection rules given in Sec. II.

REFERENCES

[1] T. P. Snow and B. J. McCall, Annu. Rev. Astron. Astrophys. **44**, 367 (2006).
[2] H. W. Kroto, Int. Rev. Phys. Chem. **1**, 309 (1981).
[3] W. Huggins, Proc. R. Soc. Lond. **33**, 1 (1882).
[4] G. Herzberg, Astrophys. J. **96**, 314 (1942).
[5] A. E. Douglas, Nature **269**, 130 (1977).
[6] W. H. Smith, T. P. Snow, and D. G. York, Astrophys. J. **218**, 124 (1977).
[7] J. P. Maier, Chem. Soc. Rev. **17**, 45 (1988).
[8] J. P. Maier, Chem. Soc. Rev. **26**, 21 (1997).
[9] J. P. Maier, J. Phys. Chem. A **102**, 3462 (1998).
[10] M. G. Giuffreda, M. S. Deleuze, J.-P. François, and A. B. Trofimov, Int. J. Quantum Chem. **85**, 475 (2001).
[11] E. B. Jochnowitz and J. P. Maier, Annu. Rev. Phys. Chem. **59**, 519 (2008).
[12] C. A. Rice and J. P. Maier, J. Phys. Chem. A **117**, 5559 (2013).
[13] W. Weltner and R. J. Van Zee, Chem. Rev. **89**, 1713 (1989).
[14] A. Van Orden and R. J. Saykally, Chem. Rev. **98**, 2313 (1998).
[15] D. Forney, P. Freivogel, M. Grütter, and J. P. Maier, J. Chem. Phys. **104**, 4954 (1996).
[16] M. Wyss, M. Grütter, and J. P. Maier, Chem. Phys. Lett. **304**, 35 (1999).
[17] S. Yang and M. Kertesz, J. Phys. Chem. A **112**, 146 (2008).
[18] R. Renner, Z. Phys. **92**, 172 (1934); G. Herzberg and E. Teller, Z. Phys. Chem. B **21**, 410 (1933).
[19] I. B. Bersuker, Chem. Rev. **113**, 1351 (2013).
[20] K. Rajak, A. Ghosh, and S. Mahapatra, J. Phys. Chem. A **122**, 8612 (2018); A. Ghosh, K. Rajak, A. K. Kanakati, and S. Mahapatra, Comput. Theor. Chem. **1155**, 109 (2019).
[21] T. H. Dunning, J. Chem. Phys. **90**, 1007 (1989).
[22] M. J. Frisch, G. W. Trucks, H. B. Schlegel, G. E. Scuseria, M. A. Robb, J. R. Cheeseman, G. Scalmani, V. Barone, B. Mennucci, G. A. Petersson, H. Nakatsuji, M. Caricato, X. Li, H. P. Hratchian, A. F. Izmaylov, J. Bloino, G. Zheng, J. L. Sonnenberg, M. Hada, M. Ehara, K. Toyota, R. Fukuda, J. Hasegawa, M. Ishida, T. Nakajima, Y. Honda, O. Kitao, H. Nakai, T. Vreven, J. A. Montgomery, Jr., J. E. Peralta, F. Ogliaro, M. Bearpark, J. J. Heyd, E. Brothers, K. N. Kudin, V. N. Staroverov, R. Kobayashi, J. Normand, K. Raghavachari, A. Rendell, J. C. Burant, S. S. Iyengar, J. Tomasi, M. Cossi, N. Rega, J. M. Millam, M. Klene, J. E. Knox, J. B. Cross, V. Bakken, C. Adamo, J. Jaramillo, R. Gomperts, R. E. Stratmann, O. Yazyev, A. J. Austin, R. Cammi, C. Pomelli, J. W. Ochterski, R. L. Martin, K. Morokuma, V. G. Zakrzewski, G. A. Voth, P. Salvador, J. J. Dannenberg, S. Dapprich, A. D. Daniels, O. Farkas, J. B. Foresman, J. V. Ortiz, J. Cioslowski, and D. J. Fox, GAUSSIAN 09 Revision E.01, Gaussian Inc., Wallingford, CT, 2009.
[23] J. M. Martin, J. El-Yazal, and J.-P. François, Chem. Phys. Lett. **252**, 9 (1996).
[24] H.-J. Werner, P. J. Knowles, G. Knizia, F. R. Manby, M. Schütz, P. Celani, T. Korona, R. Lindh, A. Mitrushenkov, G. Rauhut, K. R. Shamasundar, T. B. Adler, R. D. Amos, A. Bernhardsson, A. Berning, D. L. Cooper, M. J. O. Deegan, A. J. Dobbyn, F. Eckert, E. Goll, C. Hampel, A. Hesselmann, G. Hetzer, T. Hrenar, G. Jansen, C. Köppl, Y. Liu, A. W. Lloyd, R. A. Mata, A. J. May, S. J. McNicholas, W. Meyer, M. E. Mura, A. Nicklass, D. P. O'Neill, P. Palmieri, K. Pflüger, R. Pitzer, M. Reiher, T. Shiozaki, H. Stoll, A. J. Stone, R. Tarroni, T. Thorsteinsson, M. Wang, and A. Wolf, MOLPRO, version 2010.1, a package of *ab initio* programs, 2010, see http://www.molpro.net.
[25] E. B. Wilson, Jr., J. C. Decius, and P. C. Cross, *Molecular Vibrations* (Dover Publications, Inc., New York, 1955).
[26] H. Köppel, W. Domcke, and L. S. Cederbaum, Adv. Chem. Phys. **57**, 59 (1984).
[27] Wolfram Research, Inc., Mathematica version 8.0, Champaign, Illinois, 2010.
[28] G. Herzberg, *Molecular Spectra and Molecular Structure. III. Electronic Spectra and Electronic Structure of Polyatomic Molecules*, Molecular Spectra and Molecular Structure (Van Nostrand, 1979).
[29] A. Ghosh, S. R. Reddy, and S. Mahapatra, J. Chem. Phys. **151**, 054304 (2019).